

## Research Article

# Effect of the Passive Stabilizer Bar on the Vehicle's Stability

Duc Ngoc Nguyen <sup>1</sup>, Ngoc Duyen Dang <sup>1</sup>, Thi Thu Huong Tran <sup>2</sup>,  
Thang Binh Hoang <sup>3</sup>, and Tuan Anh Nguyen <sup>1</sup>

<sup>1</sup>Automotive Engineering Department, Thuyloi University, 175 Tay Son, Dong Da, Hanoi 100000, Vietnam

<sup>2</sup>Faculty of Vehicle and Energy Engineering, Phenikaa University, Nguyen Van Trac, Ha Dong, Hanoi 100000, Vietnam

<sup>3</sup>Hanoi University of Science and Technology, 1 Dai Co Viet, Hai Ba Trung, Hanoi 100000, Vietnam

Correspondence should be addressed to Tuan Anh Nguyen; anhngtu@tlu.edu.vn

Received 23 November 2021; Revised 29 March 2022; Accepted 25 April 2022; Published 12 May 2022

Academic Editor: Houari Ameur

Copyright © 2022 Duc Ngoc Nguyen et al. This is an open access article distributed under the Creative Commons Attribution License, which permits unrestricted use, distribution, and reproduction in any medium, provided the original work is properly cited.

The phenomenon of vehicle rollover usually occurs when the driver suddenly steers at high speed. The centrifugal force will appear and cause the vehicle's body to tilt. To overcome this situation, the solution of using the stabilizer bar is proposed. The passive stabilizer bar has a simple structure, low cost, and long service life. As a result, it is now a standard on most vehicles. This paper has established a dynamic model to describe a vehicle's oscillation. As a result of the study, the maximum roll angle of the vehicle was reduced from  $9.0^\circ$  to  $8.2^\circ$  when the stabilizer bar was used. Besides, the minimum value of the vertical force at the wheel reached 485(N) and 1162(N), respectively, corresponding to the two survey cases. The movement trajectory of the vehicle when using the stabilizer bar does not have a big difference compared to the case when the vehicle does not use the stabilizer bar. So, the vehicle's stability and safety can be effectively improved. This is the basis for further developing complex stable bar patterns in the future.

## 1. Introduction

When the vehicle moves on the road, a lot of unexpected situations can happen. In particular, the phenomenon of rollover is extremely dangerous. This phenomenon can cause extremely serious damage to passengers and cargoes.

The phenomenon of vehicle rollover usually occurs when the driver is traveling at high speed and suddenly steers. At that point, centrifugal force will appear. This force is proportional to the square of the velocity. Therefore, if the speed of the vehicle is greater, the value of the centrifugal force will also be much larger [1–3]. The centrifugal force causes the body to tilt, so the vertical force at the wheels will change. If this value is reduced to zero, i.e., the rollover index reaches the maximum threshold,  $R = 1$ , the wheel will be separated from the road surface [4, 5]. This means that the vehicle will roll over at any time [6–8]. Today, there are many methods used to limit this situation. In this case, the solution using the stabilizer bar is extremely suitable [9].

The stabilizer bar is also known as the antiroll bar, sway bar, etc. [10]. The passive stabilizer bar (mechanical) is made of steel, and it has a circular cross-section and is hollow inside. The two ends of the stabilizer bar are attached to the hub of the wheel. The back of the stabilizer bar is placed on two rubber bearings (Figure 1). It can rotate around these two positions [11]. When the body of the vehicle is tilted, the two wheels will move in opposite directions. This causes the stabilizer bar to twist. The elastic moment of the bar will help to partially eliminate the moment that causes the vehicle to roll over. From there, the stability of the vehicle will be improved more [12]. Today, stabilizer bars are fitted on passenger cars, buses, and a variety of other vehicles [13–15].

There are many methods used to calculate the impact force of the passive stabilizer bar. In [16], Vu et al. used the roll angle of the axle and the torsional stiffness of the stabilizer bar to determine the force of the bar. Besides, the method of using the displacement of the unsprung mass to calculate the force of the stabilizer bar has also been

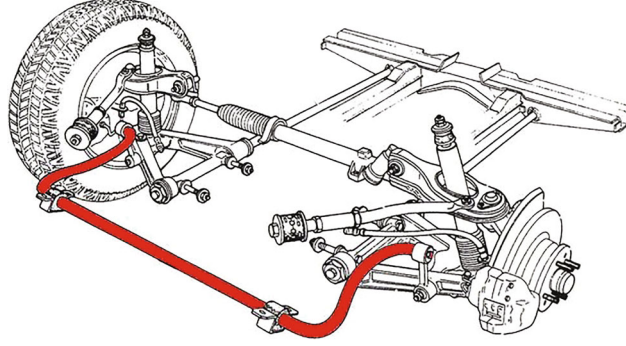


FIGURE 1: The passive stabilizer bar.

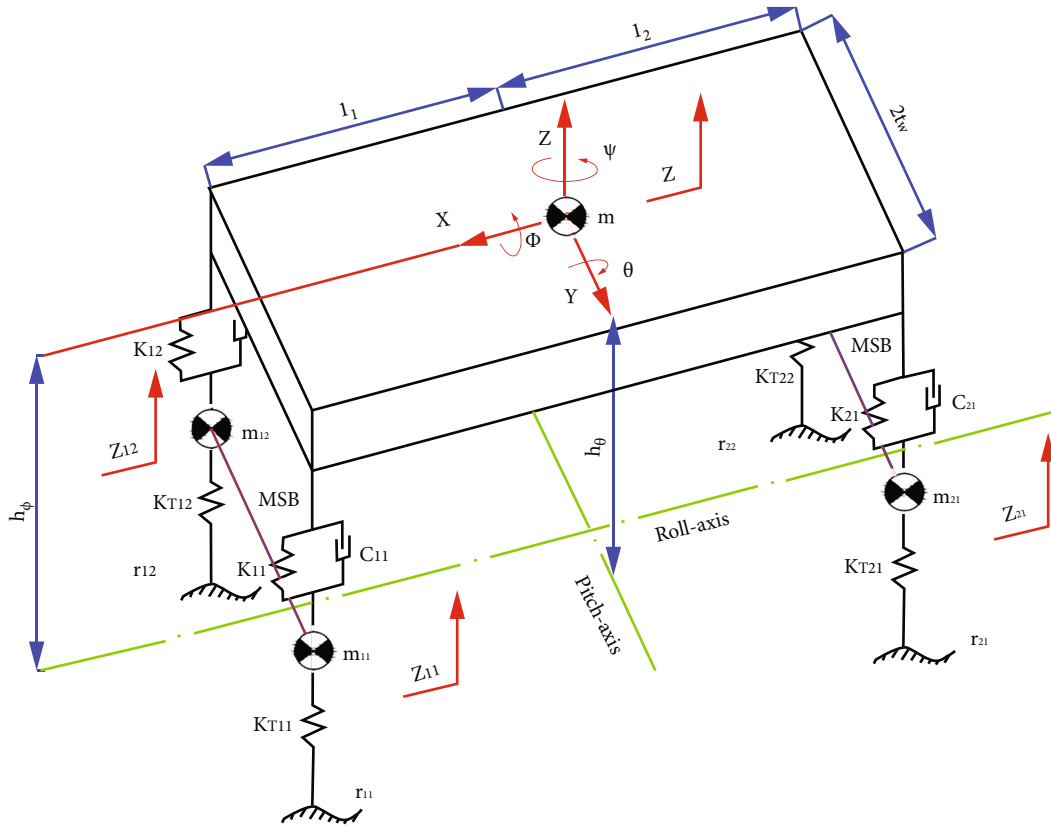


FIGURE 2: The spatial dynamics model of the vehicle.

proposed by Nguyen [17]. In some other studies, algorithms for active stabilizer bar control have also been implemented [18–21]. This paper focuses on establishing a dynamic model to describe the vehicle's oscillation when steering. At the same time, the vehicle's stability parameters such as roll angle and trajectory will be compared in the case of a vehicle using the stabilizer bar and the vehicle not using the stabilizer bar. The content of the paper is presented below.

## 2. Model of the Vehicle Dynamics

To simulate the vehicle's oscillations, a spatial dynamic model is proposed. Separating the sprung mass  $m$  and the

unsprung mass  $m_{ij}$ , this model will include 7 degrees of freedom (Figure 2).

$$\begin{aligned}
 m\ddot{z} &= \sum_{i,j=1}^2 F_{Cij} + F_{Kij}, \\
 (I_x + mh_\phi^2)\ddot{\phi} &= \sum_{i,j=1}^2 [(-1)^{i-1} (F_{Cij} + F_{Kij})t_{wi}] + a_y mh_\phi, \\
 m_{ij}\ddot{z}_{ij} &= F_{KTij} - F_{Cij} - F_{Kij} + (-1)^j F_{Si} \quad i, \quad j = \overline{1, 2}, \\
 (I_y + mh_\theta^2)\ddot{\theta} &= \sum_{i,j=1}^2 (-1)^{i-1} (F_{Cij} + F_{Kij})l_i + a_x mh_\theta,
 \end{aligned} \tag{1}$$

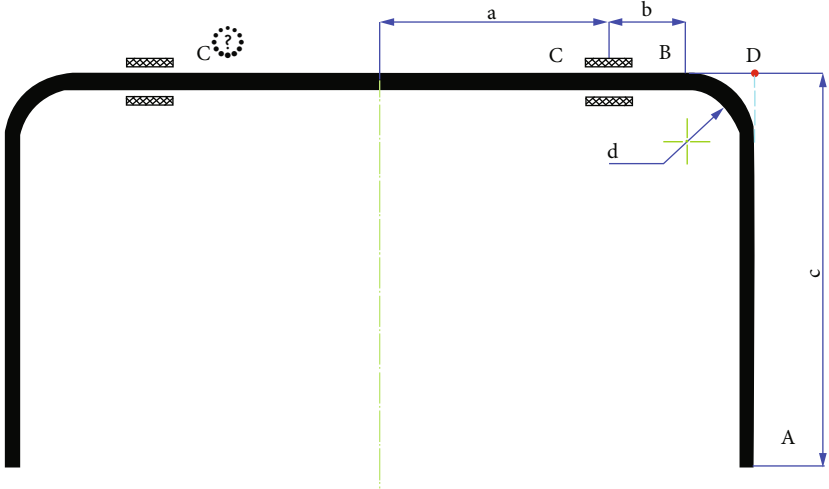


FIGURE 3: Dimensions of the passive stabilizer bar.

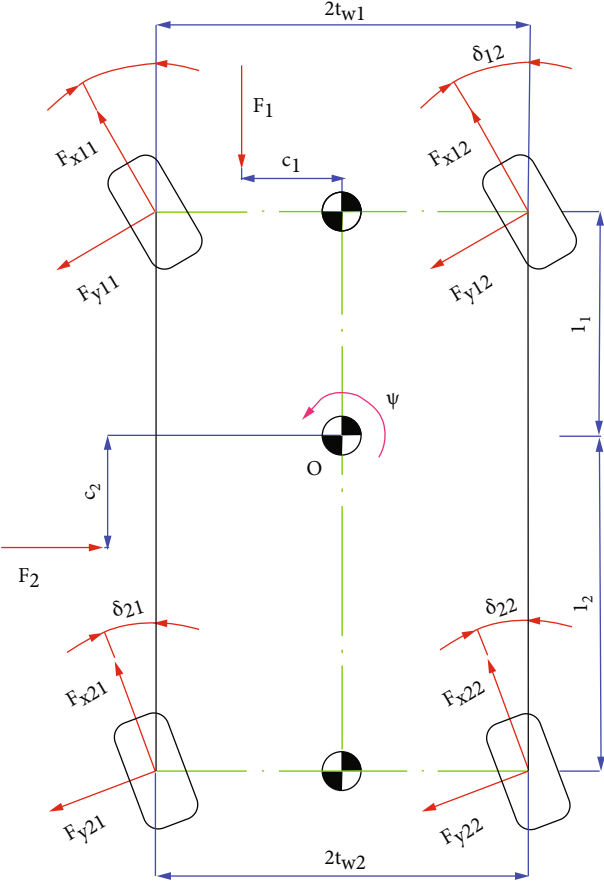


FIGURE 4: The nonlinear double-track dynamic model of the vehicle.

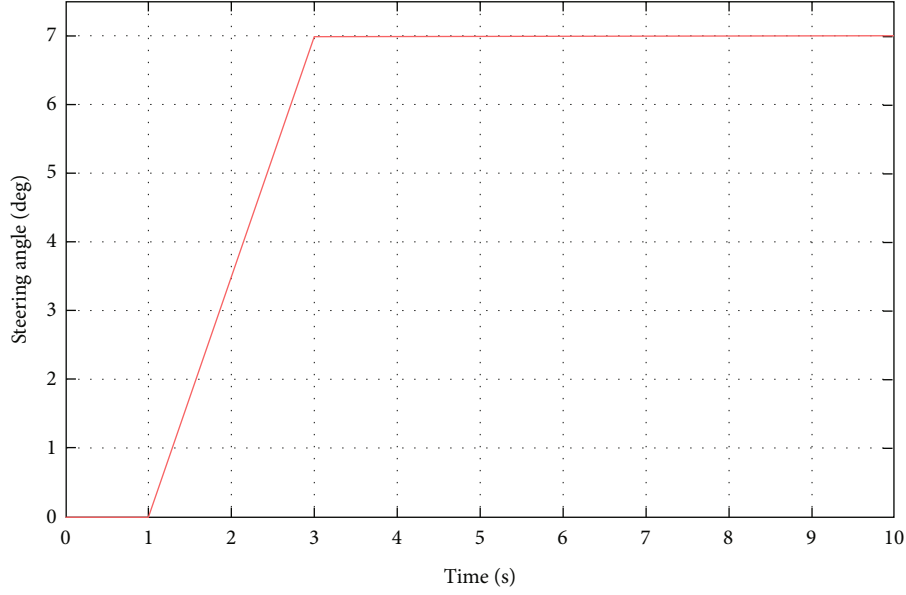


FIGURE 5: Steering angle.

TABLE 1: The technical parameters.

Description	Symbol	Value	Unit
Sprung mass	$m$	1850	kg
Unsprung mass	$m_{ij}$	50	kg
Track width	$2t_{wi}$	0.730/0.725	m
Distance from the centre of gravity to front axle	$l_1$	1.25	m
Distance from the centre of gravity to rear axle	$l_2$	1.55	m
Distance from the centre of gravity to roll axis	$h_\phi$	0.58	m
Distance from the centre of gravity to pitch axis	$h_\psi$	0.51	m
Moment of inertia of the $x$ -axis	$I_x$	710	kgm <sup>2</sup>
Moment of inertia of the $y$ -axis	$I_y$	2520	kgm <sup>2</sup>
Moment of inertia of the $z$ -axis	$I_z$	2520	kgm <sup>2</sup>
Gravitational acceleration	$g$	9.81	m/s <sup>2</sup>
Dimensions of the stabilizer bar	$a$	0.38	m
Dimensions of the stabilizer bar	$b$	0.22	m
Dimensions of the stabilizer bar	$c$	0.25	m
Dimensions of the stabilizer bar	$d$	0.1	M
Torsional stiffness coefficient	$GJ_p$	3155	Nm <sup>2</sup>
Bending stiffness coefficient	$EJ_x$	4104	Nm <sup>2</sup>

where

$$\begin{aligned}
 a_y &= g \sin \phi + \left( \dot{v}_y + (\dot{\beta} + \dot{\psi}) v_x \right) \cos \phi, \\
 \beta &= \arctan \frac{v_y}{v_x}, \\
 v_y &= v \sin \beta, \\
 v_x &= v \cos \beta.
 \end{aligned} \tag{2}$$

Because the vehicle steers at a steady speed, the longitudinal acceleration  $a_x \approx 0$ .

The equations describing the oscillations of the sprung mass are given as follows:

The impact force  $F_S$  is calculated based on the displacement of the unsprung mass as equation (Figure 3).

$$z_{ij} = \frac{F_{Si}(b+d)^3}{3EJ_x} + c \tan \int_0^{a+b} \frac{F_{Si}c}{GJ_p} dz + \frac{F_{Si}c^3}{3EJ_x}, \tag{3}$$

where

$F_S$ : The impact force generated by the passive stabilizer bar,

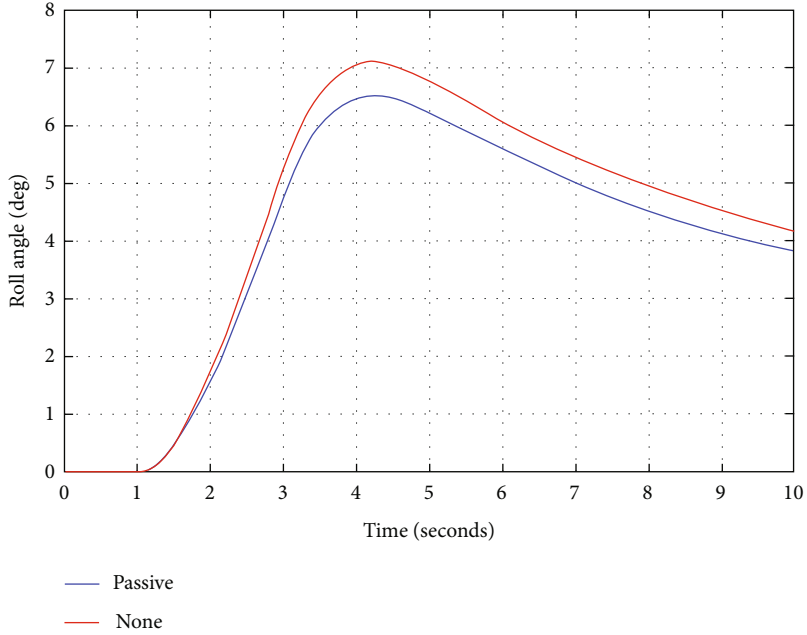


FIGURE 6: Roll angle.

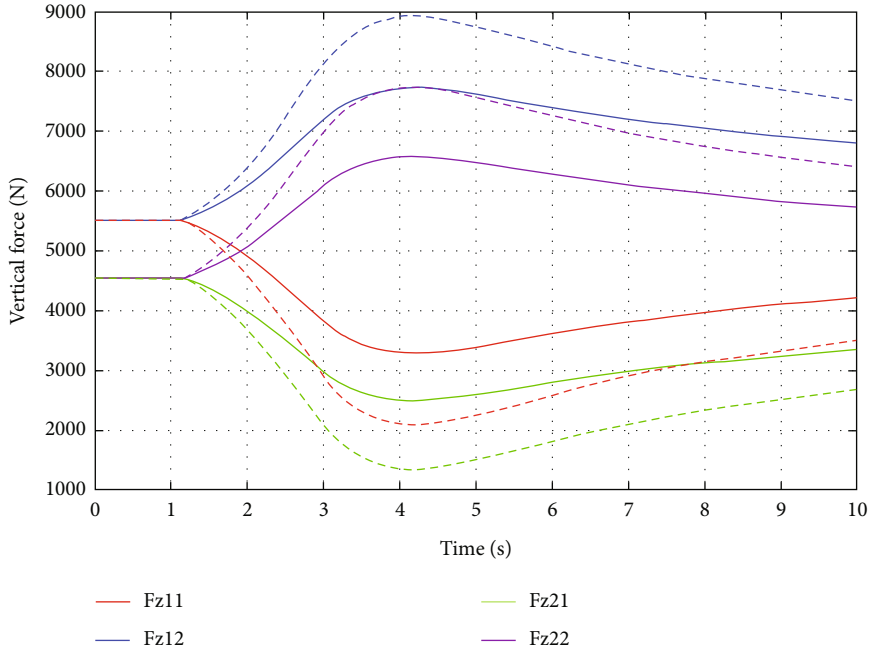


FIGURE 7: Vertical force.

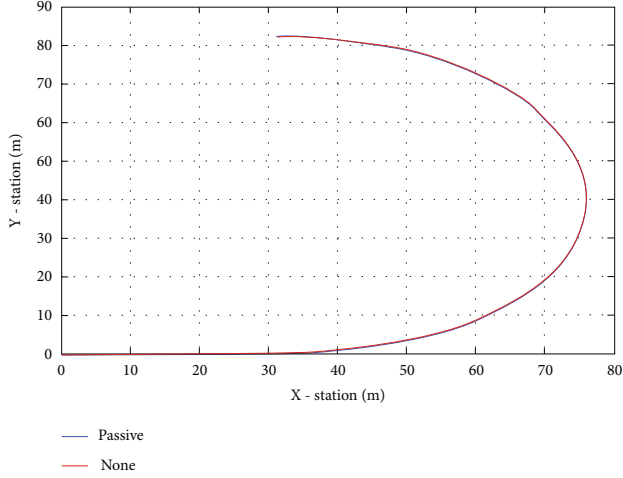


FIGURE 8: Trajectory of the vehicle.

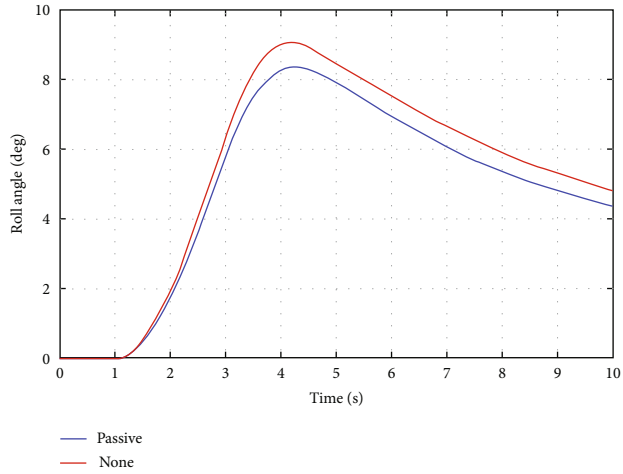


FIGURE 9: Roll angle.

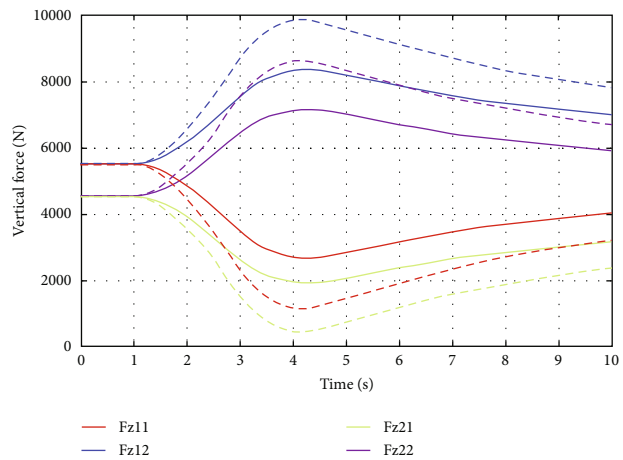


FIGURE 10: Vertical force.

a, b, c, d: Dimensions of the passive stabilizer bar,  
 $EJ_x$ : Bending stiffness of the bar,  
 $GJ_p$ : Torsional stiffness of the bar.

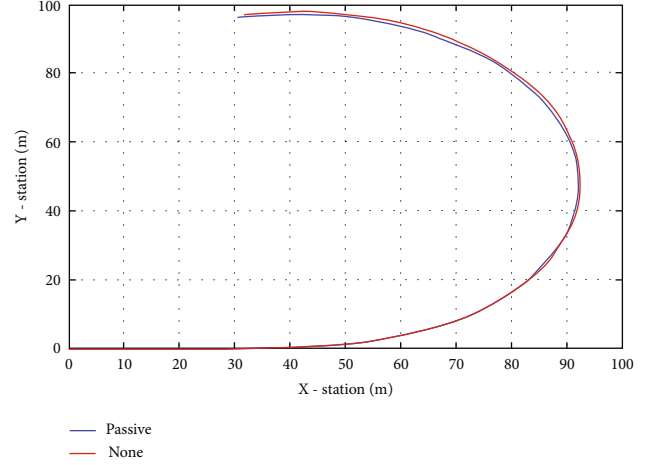


FIGURE 11: Trajectory of the vehicle.

The longitudinal and lateral velocities of the vehicle are determined based on the nonlinear double-track dynamics model (Figure 4). This model includes 3 degrees of freedom corresponding to the 3 directions of the vehicle's motion [22].

$$\begin{aligned} \left(m + \sum_{i,j=1}^2 m_{ij}\right) \left[\dot{v}_x - (\dot{\beta} + \dot{\psi})v_y\right] &= \sum_{i,j=1}^2 (F_{xij}\cos\delta_{ij} - F_{yij}\sin\delta_{ij}) - F_1, \\ \left(m + \sum_{i,j=1}^2 m_{ij}\right) \left[\dot{v}_y + (\dot{\beta} + \dot{\psi})v_x\right] &= \sum_{i,j=1}^2 (F_{xij}\sin\delta_{ij} + F_{yij}\cos\delta_{ij}) - F_2, \\ I_z \ddot{\psi} &= \sum_{i,j=1}^2 [(-1)^j (F_{xij}\cos\delta_{ij} - F_{yij}\sin\delta_{ij})l_{wi} + (-1)^{j+1} (F_{xij}\sin\delta_{ij} + F_{yij}\cos\delta_{ij})l_i + F_1 c_i - M_{zji}]. \end{aligned} \quad (4)$$

To calculate the force values at the wheel, the tire model needs to be determined. In this paper, the Pacejka tire model is proposed.

$$\begin{aligned} F_x &= D_x \sin \left\{ C_x \arctan \left[ B_x (1 - E_x) (s_x + S_{hx}) + E_x \arctan \{ B_x (s_x + S_{hx}) \} \right] \right\} + S_{vx}, \\ F_y &= D_y \sin \left\{ C_y \arctan \left[ B_y (1 - E_y) (\alpha + S_{hy}) + E_y \arctan \{ B_y (\alpha + S_{hy}) \} \right] \right\} + S_{vy}, \\ M_z &= D_z \sin \left\{ C_z \arctan \left[ B_z (1 - E_z) (\alpha + S_{hz}) + E_z \arctan \{ B_z (\alpha + S_{hz}) \} \right] \right\} + S_{vz}. \end{aligned} \quad (5)$$

The parameters of the Pacejka tire model are referenced from [23]. The type of tire used in this study was like that in [22]. There are some differences in the size specifications of the reference vehicle. However, this effect is not large.

Once all the above values have been determined, the vehicle's trajectory can be easily calculated through the coordinates of the centre of gravity in the Oxy plane.

$$\begin{aligned} X &= \int_0^t v \cos(\beta(\tau) + \psi(\tau)) d\tau, \\ Y &= \int_0^t v \sin(\beta(\tau) + \psi(\tau)) d\tau. \end{aligned} \quad (6)$$

### 3. Simulation and Result

*3.1. Simulation Condition.* Simulation is carried out when the vehicle steers at  $v_1 = 60$  (km/h) and  $v_2 = 75$  (km/h). The steering rule is shown in Figure 5. For each of the above situations, the vehicle is surveyed in two cases, including the vehicle using a passive stabilizer bar and the vehicle not using a stabilizer bar.

The technical parameters of the vehicle are given in Table 1.

#### 3.2. Result and Discussion

*Case 1.*  $v_1 = 60$  (km/h).

With speed  $v_1 = 60$  (km/h), the change of the roll angle over time is shown in Figure 6. According to this result, the maximum value of roll angle is  $6.5^\circ$  and  $7.1^\circ$ , respectively, with two case studies. After reaching the maximum value  $\phi = \phi_{\max}$ , the roll angle of the vehicle tends to decrease gradually over time.

When the roll angle of the vehicle changes, a difference in the vertical forces at the two wheels of each axle will appear. This difference depends on the roll angle (Figure 7). If the vehicle does not have a stabilizer bar, the rear wheel reaction is only 1385(N). Meanwhile, this value can be up to 2068(N) if the vehicle uses a mechanical stabilizer bar.

The determination of the vehicle's trajectory depends on the tire model used in the study. In this paper, the Pacejka tire model is proposed. According to this model, the longitudinal force  $F_x$ , the lateral force  $F_y$ , and the moment  $M_z$  are calculated based on the vertical force at the wheels  $F_{z_{ij}}$ . Therefore, when the value of the vertical force changes, the trajectory of the vehicle can also change.

According to Figure 8, the change in the vehicle's trajectory, in this case, is very small. This deviation does not exceed 1%. Therefore, the stability of the vehicle in motion is still guaranteed.

*Case 2.*  $v_2 = 75$  (km/h).

If the vehicle's speed continues to increase, more pronounced instability may occur. When the vehicle's speed reaches the value  $v_2 = 75$  (km/h), the maximum roll angle of the vehicle can be up to  $9.0^\circ$  and  $8.2^\circ$ , respectively, for the case of the vehicle without the stabilizer bar and the case of the vehicle using a mechanical stabilizer bar (Figure 9). Because the vehicle roll angle is larger than in the previous case, the change in the vertical force at the wheel is also larger (Figure 10). The value of the vertical force at position (21) is only 1162(N) and 485(N) corresponding to the two situations mentioned. If this value continues to drop to zero, the wheel will be lifted off the road. Therefore, the rollover phenomenon can happen at any time.

The change of the vertical force also causes the vehicle's trajectory to change (Figure 11). In fact, the turning radius of the vehicle when using the stabilizer bar will be smaller than when the vehicle does not use the stabilizer bar. However, this difference is not too large. Therefore, it cannot cause an oversteer phenomenon. The vehicle's motion trajectory is still guaranteed in moving situations.

### 4. Conclusions

The rollover phenomenon is a very dangerous problem. The cause of this phenomenon is the appearance of centrifugal force, which is generated when the vehicle is steering. To limit the phenomenon of vehicle rollover, the solution of using a stabilizer bar has been proposed. This paper has established a nonlinear dynamic model to describe the vehicle's oscillations when moving on the road. Two cases are considered, including the vehicle using a mechanical stabilizer and the vehicle not using a stabilizer bar. The vehicle's speed is increased to the value at which rollover is likely to occur.

The results of the study showed that when the vehicle used the stabilizer bar, the maximum roll angle of the vehicle was reduced. Besides, the difference in vertical force at the wheel is also significantly reduced. Although there is a difference in the vertical force in the two investigated cases, the vehicle's trajectory is almost unchanged. As a result, the vehicle's stability and safety have been improved.

The new study only recommends the use of a passive stabilizer bar when the vehicle is moving on the road. In many dangerous situations, the passive stabilizer bar cannot fully meet the requirements set for stability and safety for the vehicle. Therefore, solutions to improve stability, such as the use of active stabilizer bars, are required. This idea will be implemented in future studies.

### Nomenclature

$\theta$ :	Pitch angle, (rad)
$\phi$ :	Roll angle, (rad)
$\delta$ :	Steering angle, (rad)
$\psi$ :	Yaw angle, (rad)
$\beta$ :	Heading angle, (rad)
$F_i$ :	External force, (N)
$F_x$ :	Longitudinal force, (N)
$F_y$ :	Lateral force, (N)
$F_z$ :	Vertical force, (N)
$r_{ij}$ :	Roughness on the road, (m)
$v$ :	Velocity, (m/s)
$v_x$ :	Longitudinal velocity, (m/s)
$v_y$ :	Lateral velocity, (m/s)
$z$ :	Displacement of the sprung mass, (m)
$z_{ij}$ :	Displacement of the unsprung mass, (m).

### Data Availability

The data used to support this research are included within this paper.

### Conflicts of Interest

The author declares that there is no conflict of interest regarding the publication of this paper.

### References

- [1] N. T. Anh and H. T. Binh, "Determining the vertical force when steering," *Advances in Systems Science Applications*, vol. 20, no. 4, pp. 27–35, 2020.



- [2] N. T. Anh, "Predict the rollover phenomenon of the vehicle when steering," *International Journal of Mechanical & Mechatronics Engineering*, vol. 20, no. 5, pp. 31–40, 2020.
- [3] A. N. Tuan and B. H. Thang, "Research on determining the limited roll angle of vehicle," in *International Conference on Engineering Research and Applications*, pp. 613–619, 2020.
- [4] A. H. Kazemian, M. Fooladi, and H. Darijani, "Rollover index for the diagnosis of tripped and untripped rollovers," *Latin American Journal of Solids and Structures*, vol. 14, no. 11, pp. 1979–1999, 2017.
- [5] M. Ataei, A. Khajepour, and S. Jeon, "A general rollover index for tripped and un-tripped rollovers on flat and sloped roads," *Proceedings of the Institution of Mechanical Engineers, Part D: Journal of Automobile Engineering*, vol. 233, no. 2, pp. 304–316, 2017.
- [6] R. Rajamani, D. Piyabongkarn, V. Tsourapas, and J. Y. Lew, "Parameter and state estimation in vehicle roll dynamics," *IEEE Transactions on Intelligent Transportation Systems*, vol. 12, no. 4, pp. 1558–1567, 2011.
- [7] G. Phanomchoeng and R. Rajamni, "New rollover index for the detection of tripped and Untripped rollovers," *IEEE Transactions on Industrial Electronics*, vol. 60, no. 10, pp. 4726–4736, 2013.
- [8] B. Li and S. Bei, "Research method of vehicle rollover mechanism under critical instability condition," *Advances in Mechanical Engineering*, vol. 11, no. 1, 11 pages, 2019.
- [9] K. Parczewski and H. Wnek, "The influence of vehicle body roll angle on the motion stability and maneuverability of the vehicle," *Combustion Engines*, vol. 168, no. 1, pp. 133–139, 2017.
- [10] S. S. Kelkar, P. Gautam, S. Sahai, P. S. Agrawal, and R. Manoharan, "A detailed study on design, fabrication, analysis, and testing of the anti-roll bar system for formula student cars," *SN Applied Sciences*, vol. 3, no. 3, 2021.
- [11] N. T. Anh, H. T. Binh, and T. T. Tran, "Optimization of the stabilizer bar by using total scores method," *Advances in Science, Technology and Engineering Systems Journal*, vol. 5, no. 1, pp. 431–435, 2020.
- [12] T. A. Nguyen and T. B. Hoang, "Review on the stabilizer Bar equipped with the vehicle," *Journal of Mechanical Engineering Research and Developments*, vol. 44, no. 6, pp. 156–161, 2021.
- [13] W. Shi and C. Wang, *Improving light bus handling and stability by anti-roll Bar and bushing adjustment*, SAE Technical Paper, 2015.
- [14] V. Muniandy, P. M. Samin, and H. Jamaluddin, "Application of a self-tuning fuzzy PI-PD controller in an active anti-roll bar system for a passenger car," *Vehicle System Dynamics, International Journal of Vehicle Mechanics and Mobility*, vol. 53, no. 11, pp. 1641–1666, 2015.
- [15] H. Y. Hwang, T. S. Lan, and J. S. Chen, "Developing a strategy to improve handling behaviors of a medium-size electric bus using active anti-roll bar," *Symmetry*, vol. 12, no. 8, p. 1334, 2020.
- [16] V. T. Vu, O. Sename, L. Dugard, and P. Gaspar, "Enhancing roll stability of heavy vehicle by LQR active anti-roll bar control using electronic servo-valve hydraulic actuators," *Vehicle System Dynamics, International Journal of Vehicle Mechanics and Mobility*, vol. 55, no. 9, pp. 1405–1429, 2017.
- [17] T. A. Nguyen, "New methods for calculating the impact force of the mechanical stabilizer bar on a vehicle," *International Journal on Engineering Applications*, vol. 9, no. 5, 2021.
- [18] T. A. Nguyen, "Control the hydraulic stabilizer bar to improve the stability of the vehicle when steering," *Mathematical Modelling of Engineering Problems*, vol. 8, no. 2, pp. 199–206, 2021.
- [19] A. N. Tuan and B. H. Thang, "Research on dynamic vehicle model equipped active stabilizer Bar," *Advances in Science, Technology and Engineering Systems Journal*, vol. 4, no. 4, pp. 271–275, 2019.
- [20] T. A. Nguyen, "Preventing the rollover phenomenon of the vehicle by using the hydraulic stabilizer Bar controlled by a two-input fuzzy controller," *IEEE Access*, vol. 9, pp. 129168–129177, 2021.
- [21] T. A. Nguyen, "Improving the stability of the passenger vehicle by using an active stabilizer bar controlled by the fuzzy method," *Complexity*, vol. 2021, Article ID 6569298, 20 pages, 2021.
- [22] T. A. Nguyen, "Establishing the dynamics model of the vehicle using the 4-wheels steering systems," *Mathematical Modelling of Engineering Problems*, vol. 7, no. 3, pp. 436–440, 2020.
- [23] V. Muniandy, P. Mohd Samin, H. Jamaluddin, R. Abdul Rahman, and S. A. Abu Bakar, "Double anti-roll Bar hardware-in-loop experiment for active anti-roll control system," *Journal of Vibroengineering*, vol. 19, no. 4, pp. 2886–2909, 2017.